Journal of Bioenergetics and Biomembranes, Vol. 29, No. 6, 1997

Minireview: On the Structure and Gating Mechanism of the Mitochondrial Channel, VDAC

Carmen A. Mannella[1]

Received September 8, 1997

There is considerable evidence that the voltage-gated mitochondrial channel VDAC forms a β-barrel pore. Inferences about the number and tilt of β-strands can be drawn from comparisons with bacterial β-barrel pores whose structures have been determined by x-ray crystallography. A structural model for VDAC is proposed (based on sequence analysis and electron crystallography) in which the open state is like that of bacterial porins with several important differences. Because VDAC does not occur as close-packed trimers, there are probably fewer interpore contacts than in the bacterial porins. VDAC also appears to lack a large, fixed intraluminal segment and may not have as extensive a region of uniformly 35°-tilted β-strands as do the bacterial porins. These structural differences would be expected to render VDAC's β-barrel less stable than its bacterial counterparts, making major conformational changes like those associated with gating more energetically feasible. A possible gating mechanism is suggested in which movement of the N-terminal α-helix out of the lumen wall triggers larger-scale structural changes.

KEY WORDS: Porin; ion channel; mitochondria; VDAC; electron microscopy; sequence analysis; β-barrel.

INTRODUCTION

The ion channel VDAC (voltage-dependent, anion-selective channel), also called mitochondrial porin, occurs at high density in the mitochondrial outer membrane and regulates the permeability of this membrane to ions and metabolites (Colombini *et al.*, 1996; Benz, 1994; Mannella *et al.*, 1992). There is considerable evidence that VDAC, like the bacterial porins, forms a β-barrel pore. Forte *et al.* (1987) were the first to propose this, based on a pattern of alternating polar–nonpolar residues in the primary structure of VDAC from *Saccharomyces cerevisiae* (scVDAC). The amphipathic pattern suggested transmembrane β-strands with successive residues facing into an aqueous barrel lumen and into the lipid bilayer. Similar amphipathic patterns have subsequently been found in a variety of VDAC sequences, suggesting a common structural motif (Blachly-Dyson *et al.*, 1990; De Pinto *et al.*, 1991; Rauch and Moran, 1994; Song and Colombini, 1996). Additional support for a β-barrel structure has come from circular dichroism studies. Far-UV CD spectra of VDAC from *Neurospora crassa* (ncVDAC) are similar to those of bacterial porins and indicate considerable β-sheet secondary structure (Shao *et al.*, 1996). However, despite the apparent structural similarities with bacterial porins, VDAC has an important functional distinction, i.e., it undergoes reversible, low-voltage-induced partial closures not seen with the porins. Occupancy of these "closed" states, which are impermeable to ATP (Benz *et al.*, 1990; Liu and Colombini, 1992; Rostovtseva and Colombini, 1996), is favored by certain polyanions (Colombini *et al.*, 1987) and endogenous effectors, NADH (Zizi *et al.*, 1994) and a soluble mitochondrial protein (Holden and Colombini, 1993), suggesting that the states may be occupied by VDAC in its mitochondrial environment. There is considerable evidence that closure of VDAC involves major re-arrangements of the pore structure (Peng *et al.*, 1992; Colombini *et al.*, 1996) that are difficult to reconcile with porin-like β-barrels, which are highly stable structures.

[1] Division of Molecular Medicine, Wadsworth Center, New York State Department of Health, Albany New York 12201–0509; and Department of Biomedical Sciences, School of Public Health, University at Albany (SUNY), Albany, New York.

0145-479X/97/1200-0525$12.50/0

In this review, information about VDAC derived from sequence analysis employing the Gibbs sampler (Lawrence *et al.*, 1993) and from electron microscopy of two-dimensional crystals is shown to provide a conceptual framework for understanding several functional characteristics of the mitochondrial pore relative to bacterial porins, whose atomic structures have been determined by x-ray crystallography.

STRUCTURAL INFORMATION ABOUT VDAC

Diameter of the VDAC Pore

Direct physical measurement of the size of the VDAC pore has been provided by cryo-electron microscopy of frozen-hydrated two-dimensional crystals of fungal VDAC. The crystals are obtained by phospholipase/dialysis treatment of isolated mitochondrial outer membranes (Mannella, 1984) and are imaged after fast-freezing in buffer without stain or chemical fixation. High-resolution correlation-averaged images of the crystals indicate that the mean diameter of VDAC's pore at the Cα backbone is 3.6–3.8 nm (Mannella *et al.*, 1989; Guo and Mannella, 1993), consistent with the permeability of the open channel to ions and uncharged polymers (Mannella *et al.*, 1992).

Knowing this diameter and the geometry of ideal and actual β-barrel pores, upper and lower limits can be put on the number of transmembrane β-strands in the VDAC pore (Mannella *et al.*, 1992). For example, heptamers of the bacterial toxin α-hemolysin form a transmembrane β-barrel with 14 β-strands uniformly tilted about 35° with respect to the barrel axis (Song *et al.*, 1996). (This is referred to as a "35°-β" fold in what follows.) The Cα diameter of the circular α-hemolysin β-barrel is 2.8 nm. Typical bacterial porins (such as *R. capsulatus* porin, and *E. coli* OmpF and PhoE) form β-barrels with roughly elliptical cross-sections and mean diameters of about 3.4 nm (Weiss *et al.*, 1991; Cowan *et al.*, 1992). This is much wider than the α-hemolysin β-barrel even though the porins contain only two more transmembrane β-strands. The reason for the disproportionately wider porin pores is that only 11 of their 16 β-strands are tilted at 35°. The other 5 transverse strands have a considerably greater tilt, 45–60°. In order for VDAC to have a Cα diameter wider than the bacterial porins', it must contain more than 16 transmembrane strands and/or a larger proportion of the strands must be tilted well past 35°. If the barrel were composed of only 13 transmembrane segments, as proposed by one group (Blachly-Dyson *et al.*, 1990), all the strands would have to be tilted at about 60° to form a pore with Cα diameter of 3.8 nm.

Evidence for Structural Domains within the VDAC Protein

An analysis of multiple VDAC sequences employing the Gibbs sampler (Lawrence *et al.*, 1993) has provided additional clues about the structure of this channel (Mannella *et al.*, 1996). Numerous matches were found in six different VDAC sequences to two closely related residue frequency motifs (11 and 13 residues in length) previously discovered in a search of bacterial outer-membrane protein sequences (Neuwald *et al.*, 1995). The bacterial motifs had been determined to correspond to transmembrane β-strands in porins of known structure, specifically to β-strands in contact with lipid and tilted 35°.

Table I summarizes the 11-residue bacterial motif and the corresponding residue frequencies in the mitochondrial subsequences that matched the motif. As expected for transmembrane β-strands, the motif contains an alternating polar–nonpolar pattern at positions 3–11. Positions 1–2 are predominantly polar and probably correspond to residues that interact with the phospholipid headgroup region of the bilayer. At even (lumen-facing) residue positions, glycine predominates in the middle of the motif, while charged residues are more frequent at the ends. At odd (lipid-facing) positions, aliphatic residues tend to fall in the middle and aromatics at the ends of the motif. A horizontal "banding" of charged and aromatic residues predicted by this residue pattern is, in fact, observed in the atomic structures of individual bacterial porins (Weiss and Schulz, 1992; Cowan *et al.*, 1992) and, based on the results of Table I, likely also occurs in VDAC.

The subsequences in VDAC that match the bacterial porin motifs fall in two clusters along the polypeptide sequence, at residues 77–155 and 200–281. (The residue-numbering system corresponds to scVDAC.) Since the regions in bacterial porin sequences associated with the motifs correspond to transmembrane β-strands in contact with lipid and tilted 35°, the same is probably true of the two regions identified in the VDAC sequences. This suggests that VDAC may have at least four distinct structural domains (Fig. 1), two of which (residues 77–155 and 200–281) have the "35°-β" fold. The other two regions (residues 1–76 and 156–199) may

Table I. Residue Frequency Pattern Found by Gibbs Sampler Analysis of Bacterial and Mitochondrial Pore-Forming Polypeptides[a]

	Frequency of occurrence at indicated residue position										
Residue class	1	2	3	4	5	6	7	8	9	10	11
Small, apolar						28		37			
(G)						(55)		(35)			
Polar, uncharged	15	47				21		15			
(S,T,N,Q)	(55)	(35)				(30)		(15)			
Polar, charged	46									43	
(D,E,K,R,H)	(20)									(40)	
Nonpolar, aliphatic					59		68		38		
(A,V,I,L,M)					(75)		(60)		(40)		
Aromatic			42		15				35		73
(W,Y,F)			(0)		(25)				(20)		(85)

[a] Top numbers are the percent occurrence of a given class of residues at the corresponding position in the 11-residue motif derived from Gibbs sampler analysis of bacterial porin sequences. (Class frequencies below 15% are not indicated.) Bottom numbers in parentheses are the corresponding residue frequencies in the mitochondrial polypeptide segments found to match the bacterial motif. Note that the only major discrepancy is the absence of aromatic residues at position 3 in the mitochondrial segments. (Results summarized from Neuwald *et al.*, 1995 and Mannella *et al.*, 1996.)

consist in part of β-sheet regions in which strands are tilted more obliquely, and/or they may have non-β structure, i.e., loops or α-helices.

Electron microscopy of frozen-hydrated and gold-glucose-embedded VDAC crystals also indicates that there are discrete structural domains in VDAC (Mannella *et al.*, 1989; Guo *et al.*, 1995). The projected profile of the pore is not circular like α-hemolysin but instead is tetragonal (Fig. 2A). Consistent with the projected views, three-dimensional reconstruction of VDAC shows that its lumen is composed over most of its length of four flat or gently curved sides (Fig. 2B). In bacterial porins, there is a clear difference in the shape of the lumen wall between the continuous "35°-β" region (which is curved) and the β-sheet region with more obliquely tilted strands (which is flatter) (Weiss *et al.*, 1991; Cowan *et al.*, 1992). This suggests that the four sides of VDAC's lumen may correspond to four domains of discrete secondary structure, as inferred above from the Gibbs sampler analysis.

Another recognizable structural domain in the VDAC protein is a lateral arm that extends between the pores in one class of VDAC crystals (Mannella *et al.*, 1989; Guo and Mannella, 1993) and is labeled by antibodies against residues 1–20 (Guo *et al.*, 1995). There is evidence from sequence analysis (Kleene *et al.*, 1987) and circular dichroism (Guo *et al.*, 1995) that residues 1–20 may fold as an amphipathic α-helix. Therefore, it is likely that the arm in the crystal images represents an N-terminal α-helix located outside VDAC's pore.

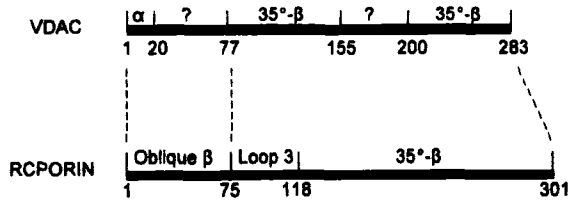

Fig. 1. Structural domains within the sequences of bacterial porin (rcPorin), determined by x-ray crystallography (Weiss *et al.*, 1991), and of mitochondrial VDAC, predicted by the Gibbs sampler (Mannella *et al.*, 1996).

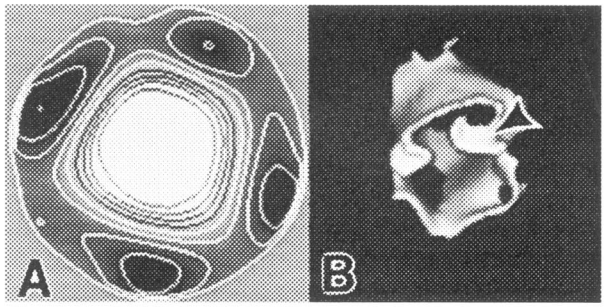

Fig. 2. Four-sided shape of the pore defined by fungal VDAC. (**A**) Projected density map of the lumen (white) in frozen-hydrated 2D crystals of ncVDAC. Outer circular profile is a mask (diameter = 4.3 nm) used in image processing and does not represent the outer shape of the pore. (Figure reproduced from Guo *et al.*, 1995 with permission of Academic Press) (**B**) Three-dimensional shape of the inner wall of the pore of fungal VDAC embedded in gold-glucose. Arrow points to flap in lumen wall (see Fig. 3).

COMPARISON OF THE STRUCTURES OF VDAC AND BACTERIAL PORINS

In Fig. 3, the Cα backbone of *R. capsulatus* porin (rcPorin) derived from x-ray crystallography (Weiss and Schulz, 1992) is superimposed on an outline of the VDAC lumen derived from three-dimensional reconstruction of the 2D crystals (Guo *et al.*, 1995). In the figure, the binding site on VDAC for the N-terminal antibody is aligned with the N-terminus in rcPorin. Using this alignment, the rcPorin backbone fits surprisingly well inside VDAC's outline, with a few exceptions. One is that VDAC has a larger circumference than rcPorin, consistent with its greater mean diameter. A second difference is a flap-like region in the VDAC lumen which aligns with a special domain in the bacterial porin called loop 3. (The flap is indicated by an arrow in Fig. 2B.) Loop 3 is a 40-residue segment between two adjacent β-strands that extends inside the pore and interacts with residues in the lumen wall. There is no evidence in electron micrographs of frozen-hydrated VDAC crystals for a similar obstruction in the mitochondrial pore (Mannella *et al.*, 1989; Guo and Mannella, 1993; also Mannella, unpublished results). On the contrary, there is a groove (absence of mass) in the wall of VDAC's lumen that, in effect, defines the flap (Figs. 2B and 3) and extends an additional 2 nm around the lumen at an oblique angle (Guo *et al.*, 1995).

Another significant structural difference between VDAC and bacterial porins is that the latter form symmetrical trimeric complexes with numerous contacts between β-barrels (indicated in Fig. 3) in the regions where the β-strands are tilted beyond 35°. VDAC pores do not assemble as close-packed symmetrical trimers in 2D crystals (Mannella and Guo, 1992) and so should lack extensive stabilizing interpore contacts. This is consistent with the relative ease of denaturing the secondary structure of VDAC relative to bacterial porins (Shao *et al.*, 1996).

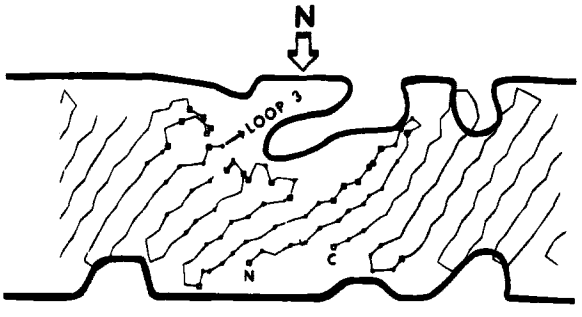

Fig. 3. Superposition of the Cα backbone of rcPorin (reproduced from Weiss and Schulz, 1992 with permission of the author and Academic Press) on the cylindrical projection of the lumen wall of VDAC (Guo *et al.*, 1995). Arrow points to the position along the VDAC lumen closest to the binding site of the N-terminal antibody. This is also near the position of the flap and groove in the lumen (see Fig. 2B). Residues marked by boxes and dots in the rcPorin backbone are those involved in forming intersubunit contacts.

A PORIN-LIKE STRUCTURAL MODEL FOR VDAC

The above structural comparisons suggest that the mitochondrial channel VDAC and the class of bacterial porins represented by rcPorin, OmpF, and PhoE may be closely related, perhaps even derived from a common proto-β-barrel membrane protein. Furthermore, it is possible to speculate how the two classes of pores may have diverged structurally such that VDAC functions as a gated, relatively nonselective, monomer channel, while the bacterial porins are stable, ion-selective, trimeric channels.

Number and orientation of β-strands: In the C-terminal three-fourths of the pore-forming polypeptides, where the bacterial porins have an uninterrupted region of eleven antiparallel β-strands tilted 35°, VDAC may have two shorter "35°-β" regions (Fig. 1), as suggested by the Gibbs sampler analysis described above. Region 77–155 in VDAC contains six unique matches to the bacterial motif, and region 200–201 contains five, suggesting that there are at least eleven transmembrane β-strands in the two regions. A sixth amphipathic β-strand may also occur in region 200–281 based on an alternating polar–nonpolar pattern at residues 228–238 (De Pinto *et al.*, 1991; Rauch and Moran, 1994). The N-terminal region of VDAC (except for residues 1–20) may fold primarily as obliquely tilted β-strands as does the N-terminal region of bacterial porins. As many as four amphipathic transmembrane β-strands may occur between residues 21–76 based on patterns of alternating polar–nonpolar residues in this region (Blachly-Dyson *et al.*, 1990). Likewise, at least two amphipathic β-strands may be assigned to the non-35°-β region containing residues 156–199 (Rauch and Moran, 1994). These assignments yield a β-barrel with as many as twelve β-strands tilted 35° and another six β-strands with a more oblique tilt, consistent with VDAC's pore diameter being a little wider than that of the bacterial porins, which have

eleven β-strands tilted 35° and five tilted more obliquely. Note that such an 18-strand β-barrel allows for very few segments longer than 3–4 residues outside the β-barrel. Not counting the N-terminal α-helix, the longest putative non-β regions occur at residues 99–107 and 156–174.

No intraluminal segment: The structural superposition in Fig. 3 suggests that loop 3 in rcPorin and the "flap" in VDAC may represent analogous domains, flipped inside and occluding the bacterial pore, and instead forming part of the external wall of the mitochondrial pore. Loop 3, like equivalent domains in other bacterial porins, defines the major selectivity filter of these porins and probably also acts to rigidify the β-barrel (Cowan *et al.*, 1992; Weiss and Schulz, 1992). The absence of a large, obstructing, internal loop would explain VDAC's greater maximum permeability and lower ion selectivity relative to bacterial porins (Table II). The most likely candidates to form the flap in VDAC are the two non-β, non-α regions noted in the previous paragraph.

Less stable "open" state: Several structural factors noted above may make VDAC's β-barrel considerably less stable than that of its bacterial counterparts. First, the mitochondrial β-barrels do not form close-packed trimers (Mannella and Guo, 1992) and so should lack stabilizing intersubunit contacts like those that occur within the bacterial porin complex. Second, VDAC appears to lack a fixed internal loop 3-like domain, which serves to rigidify as well as constrict the bacterial β-barrels. Lastly, unlike the bacterial porins which have a continuous 11-strand "35°-β" domain, the Gibbs sampler results suggest that VDAC has two shorter such regions interrupted by residues 156–199. The latter domain and/or the N-terminal region may contain one or more sites at which interstrand H-bonding is less extensive than in the "35°-β" domains, making disruption of the β-barrel more energetically feasible.

Table II. Comparison of Ion-Channel Properties of Bacterial and Mitochondrial Pores

Pore	Λ[a] (nS)	P_c/P_a[b]
E. coli OmpF[c]	2.1	3.9
E. coli PhoE[d]	1.8	0.30
Rat liver VDAC		
"Open"[e,f]	4.3	0.59
"Closed"[e,g]	2.4	~10

[a] Single-channel conductances in 1 M KCl.
[b] Ratios of cation to anion permeabilities calculated from zero-current potentials in KCl gradients of 10 mM vs. 100 mM, except for "closed" VDAC for which the gradient was 50 mM vs 320 mM KCl.
[c] Benz *et al.*, 1985.
[d] Benz *et al.*, 1984.
[e] Benz *et al.*, 1990.
[f] Roos *et al.*, 1982.
[g] Parameters measured in the presence of 16 μM modulator polyanion.

IMPLICATIONS FOR CHANNEL GATING

Evidence for Conformation Changes

VDAC, unlike bacterial porins, exhibits transitions to partially closed states in the presence of small transmembrane voltages. It is interesting that VDAC's partially closed states are similar in ionic conductance and selectivity to the "open" states of bacterial porins (Table II). This suggests that some "closed" states of VDAC might correspond to partial occlusion of the pore by movement of external domains (like the flap or N-terminal α-helix) into the β-barrel (Mannella, 1990). However, there is growing evidence that the best characterized "closed" state of VDAC represents a more significant rearrangement of the pore itself, possibly involving the removal of large sections of polypeptide from the wall of the β-barrel (Peng *et al.*, 1992).

As noted above, there is reason to believe that VDAC's β-barrel may be considerably less stable than that of the bacterial porins, making large-scale, low-energy conformational changes feasible in principle. There is also experimental evidence supporting the existence of multiple conformers of the channel protein. Circular dichroism studies of Shao *et al.* (1996) indicate that VDAC can undergo a reversible pH-dependent conformational change resulting in reduction of β-sheet content and concomitant loss of channel activity (Shao *et al.*, 1996). Also, the C-terminal segment of the VDAC polypeptide, which is a consensus transmembrane β-strand (Blachly-Dyson *et al.*, 1990; De Pinto *et al.*, 1991; Rauch and Moran, 1994; Mannella *et al.*, 1996), is purported to leave the lumen wall during closure (Peng *et al.*, 1992). This same segment in ncVDAC is at least partly accessible to antibodies in isolated mitochondria (Stanley *et al.*, 1995), suggesting that a conformer of the pore protein corresponding to a "closed" state may occur in the mitochondrial outer membrane.

A Hypothetical Gating Mechanism

The group that first proposed that gating of VDAC may involve removal of transmembrane strands from the β-barrel identified the moving segments based on relative effects of point mutations on VDAC's ion selectivity (reversal potential) in the "open" and "closed" states (Peng *et al.*, 1992). They also identified putative voltage-sensing regions in the polypeptide through the effects of point mutations on the steepness of the voltage dependence (Thomas *et al.*, 1993). Since there is only partial correspondence between the two classes of residues, they have concluded that the gating process may be complex (Colombini *et al.*, 1996).

One possibility is that VDAC's gating process occurs in steps, i.e., that a change in transmembrane potential induces movement of one or more voltage sensors which triggers subsequent larger-scale rearrangements. A likely mobile region in VDAC is the N-terminal amphipathic α-helix which, as noted above, forms an arm that extends away from the pore in one crystalline state (Mannella *et al.*, 1989; Guo and Mannella, 1993) but which appears to be part of the lumen wall in the open state observed in bilayers (Blachly-Dyson *et al.*, 1990). It is interesting that the pronounced groove in the lumen wall of crystalline VDAC occurs in the vicinity of the N-terminal domain (Guo *et al.*, 1995). It may be that, in the "open" state of VDAC, the N-terminal arm normally resides in this groove, which extends about halfway across the bilayer at an oblique angle. The arm would not create an occlusion (like loop 3 of bacterial porins) but would form part of the wall itself, similar to the proposal of Blachly-Dyson *et al.* (1990). If the N-terminal α-helix were to leave the groove in response to a stimulus (change in voltage, binding of modulator), this might seriously destabilize the β-barrel (e.g., by reducing interstrand bonding and/or by exposing the aqueous contents of the pore to the hydrophobic interior of the bilayer), making a different conformation more energetically favored. In this scenario, the channel conformation in the 2D crystal (an open pore with the α-helix outside the groove) might represent a metastable intermediate trapped by lattice forces not present (or much reduced) in the normal outer membrane.

Several different kinds of evidence lend credence to this hypothetical gating mechanism. First, mutations at several positions within residues 1–20 of scVDAC alter voltage dependence, suggesting that the N-terminal domain functions as a voltage sensor (Thomas *et al.*, 1993). Also, truncation of the first 8 residues in scVDAC causes loss of voltage dependence and instability of the open state of the channel (Koppel *et al.*, 1997 and manuscript in preparation; also *cf.* Popp *et al.*, 1996), consistent with involvement of the N-terminal domain in both voltage sensing and lumen wall formation. Finally, there is a class of "contracted" VDAC crystals in which the N-terminal arm does not extend laterally away from the pore and the projected density of the lumen wall is altered (Guo and Mannella, 1993; Mannella, 1997), consistent with movement of one or more domains between the lumen wall and the bilayer surface.

PROSPECTS FOR THE FUTURE

Work is ongoing in several laboratories aimed at providing detailed new information about the topology of the VDAC pore in phospholipid bilayers and in the mitochondrial outer membrane (e.g., Zizi *et al.*, 1995; Stanley and Mannella, 1997). Attempts to improve the quality of 2D crystals of VDAC and to grow 3D crystals (for x-ray crystallography) are also under way using bacterially expressed protein (Koppel *et al.*, 1997), and the outcome may be improved resolution of the VDAC pore in one or more conformational states. The new data should help to sort between features of the "porin-like" VDAC model proposed here and those of other models, e.g., that of Blachly-Dyson *et al.* (1990) which is largely derived from site-directed mutagenesis of scVDAC. The expectation (or at least the hope) is that evolving models will converge on a consensus structure that will fully account for the functional characteristics of this interesting and important channel protein.

ACKNOWLEDGMENTS

This work is supported by grant MCB-9506113 from the National Science Foundation and uses the facilities of the Wadsworth Center's Biological Microscopy and Image Reconstruction Resource, supported by grant RR01219 from the National Institutes of Health Biomedical Resource Technology Program (NCRR, DHHS/PHS) and by grant BIR-9219043 from the National Science Foundation.

REFERENCES

Benz, R. (1994). *Biochim. Biophys. Acta* **1197**, 167–196.

Benz, R., Darveaux, R. P., and Hancock, R. E. W. (1984). *Eur. J. Biochem.* **140**, 319–324.

Benz, R., Schmid, A., and Hancock, R. E. W. (1985). *J. Bacteriol.* **162**, 722–727.

Benz, R., Kottke, M., and Brdiczka, D. (1990). *Biochim. Biophys. Acta* **1022**, 311–318.

Blachly-Dyson, E., Peng, S. Z., Colombini, M., and Forte, M. (1990). *Science* **247**, 1233–1236.

Colombini, M., Yeung, C. L., Tung, J., and König, T. (1987). *Biochim. Biophys. Acta* **905**, 279–286.

Colombini, M., Blachly-Dyson, E., and Forte, M. (1996). In *Ion Channels*, Vol. 4, Plenum Press, New York, pp. 169–202.

Cowan, S. W., Schirmer, T., Rummel, G., Steiert, M., Ghosh, R., Pauptit, R. A., Jansonius, J. N., and Rosenbusch, J. P. (1992). *Nature* **358**, 727–733.

De Pinto, V., Prezioso, G., Thinnes, F., Link, T. A., and Palmieri, F. (1991). *Biochemistry* **30**, 10191–10200.

Forte, M., Guy, H. R., and Mannella, C. A. (1987). *J. Bioenerg. Biomembr.* **19**, 341–350.

Guo, X. W., and Mannella, C. A. (1993). *Biophys. J.* **64**, 545–549.

Guo, X. W., Smith, P. R., Cognon, B., D'Arcangelis, D., Dolginova, E., and Mannella, C. A. (1995). *J. Struct. Biol.* **114**, 41–59.

Holden, M. J., and Colombini, M. (1993). *Biochim. Biophys. Acta* **1144**, 396–402.

Kleene, R., Pfanner, N., Pfaller, R., Link, T., Sebald, W., Neupert, W., and Tropschug, M. (1987). *EMBO J.* **6**, 2627–2633.

Koppel, D. A., Kinnally, K. W., and Mannella, C. A. (1997). *Biophys. J.* **72**, A38.

Lawrence, C. E., Altschul, S. F., Boguski, M. S., Liu, J. S., Neuwald, A. F., and Wootton, J. C. (1993). *Science* **262**, 208–214.

Liu, M. Y., and Colombini, M. (1992). *Biochim. Biophys. Acta* **1098**, 255–260.

Mannella, C. A. (1984). *Science* **224**, 165–166.

Mannella, C. A. (1990). *Experientia* **46**, 137–145.

Mannella, C. A. (1997). In *Proc. Microscopy and Microanalyas 1997*, Springer Verlag, New York, pp. 1065–1066.

Mannella, C. A., and Guo, X. W. (1992). *Trans. ACA* **28**, 176–182.

Mannella, C. A., Guo, X. W., and Cognon, B. (1989). *FEBS Lett.* **253**, 231–234.

Mannella, C. A. Forte, M., and Colombini, M. (1992). *J. Bioenerg. Biomembr.* **24**, 7–19.

Mannella, C. A., Neuwald, A. F., and Lawrence, C. E. (1996). *J. Bioenerg. Biomembr.* **28**, 161–167.

Neuwald, A. F., Liu, J. S., and Lawrence, C. E. (1995). *Protein Sci.* **4**, 1618–1632.

Peng, S., Blachly-Dyson, E., Forte, M., and Colombini, M. (1992). *Biophys. J.* **62**, 123–135.

Popp, B., Court, D. A., Benz, R., Neupert, W., and Lill, R. (1996). *J. Biol. Chem.* **271**, 13593–13599.

Rauch, G., and Moran, O. (1994). *Biochem. Biophys. Res. Commun.* **200**, 908–915.

Roos, N., Benz, R. and Brdiczka, D. (1982). *Biochim. Biophys. Acta* **686**, 204–214.

Rostovtseva, T., and Colombini, M. (1996). *J. Biol. Chem.* **271**, 28006–28008.

Shao, L., Kinnally, K. W., and Mannella, C. A. (1996). *Biophys. J.* **71**, 778–786.

Song, J., and Colombini, M. (1996). *J. Bioenerg. Biomembr.* **28**, 153–161.

Song, L., Hobaugh, M. R., Shustak, C., Cheley, S., Bayley, H., and Gouaux, J. E. (1996). *Science* **274**, 1859–1866.

Stanley, S., and Mannella, C. A. (1997). *Biophys. J.* **72**, A347.

Stanley, S., Dias, J. A., D'Arcangelis, D., and Mannella, C. A. (1995). *J. Biol. Chem.* **270**, 16694–16700.

Thomas, L., Blachly-Dyson, E., Colombini, M., and Forte, M. (1993). *Proc. Natl. Acad. Sci. USA* **90**, 5446–5449.

Weiss, M. S., and Schulz, G. E. (1992). *J. Mol. Biol.* **227**, 493–509.

Weiss, M. S., Kreusch, A., Schiltz, E., Nestel, U., Welte, W., Weckesser, J., and Schulz, G. E. (1991). *FEBS Lett.* **280**, 379–382.

Zizi, M., Forte, M., Blachly-Dyson, E., and Colombini, M. (1994). *J. Biol. Chem.* **269**, 1614–1616.

Zizi, M., Thomas, L., Blachly-Dyson, E., Forte, M., and Colombini, M. (1995). *J. Membr. Biol.* **144**, 121–129.